AoI-Aware Adaptive Relaying in Buffer-Aided Wireless-Powered NOMA Network with Random Arrivals

Shi Zhou, Qingchun Chen, Yaxuan Chen, Lei Zheng
School of Electronics and Communication Engineering, Guangzhou University, Guangzhou, 510006, China.
Email: 2112130010@e.gzhu.edu.cn, qcchen@gzhu.edu.cn, chenyaxuancyx@126.com, lzheng@gzhu.edu.cn.

***Abstract*—In this paper, we considered an age of information(AoI)-aware adaptive relaying scheme in buffer-aided wireless powered non-orthogonal multiple access(NOMA) network, where one buffer-aided source node is supposed to deliver two data streams to two destination nodes with the help of one buffer-aided relay node. Meanwhile, the data streams for two destination nodes are independently and randomly generated. The buffer-aided relay node is supposed to provide energy to source node through wireless energy harvesting technology, and forward two data streams received from source node to two destination nodes through downlink NOMA technology. For this buffer-aided wireless powered NOMA network, the long-term weighted average AoI minimization problem was formulated. By using Lyapunov optimization framework and subdividing the long-term weighted average AoI minimization problem into multiple subproblems, we obtain an adaptive AoI-aware relaying scheme for buffer-aided wireless powered NOMA network. Our analysis results indicate that, by adaptively adjusting the transmission rate, transmission powers, and optimizing the selection of appropriate transmission modes, the long-term weighted average AoI performance at two destination nodes can be optimized. In addition, numerical analysis results show that the proposed AoI-aware adaptive relaying scheme provides an effective relaying scheme for buffer-aided wireless powered NOMA relay network.**

***Index Terms*—AoI-aware Adaptive Scheduling, Buffer-aided NOMA Relay Network, Random Arrivals.**

I. Introduction

With the continuous advancement of technologies such as 5G, the Internet of Things (IoT) has experienced explosive growth in recent years. Because of its higher speeds, lower latency, and greater capacity, 5G technology is driving digital transformation in various industries and vigorously promoting applications such as smart cities, autonomous vehicles, remote healthcare, and the IoT. There are a large number of real-time sensing and monitoring tasks in IoT applications, in which the freshness of information plays a crucial role. For example, in autonomous vehicles, unmanned aerial vehicles (UAVs), and industrial control networks, devices need to receive control commands from the control center in a timely manner to ensure normal system operation. An increasing number of studies have adopted the AoI as a metric to characterize the timeliness of information[1]-[3]. AoI is a receiver-centric metric that captures the elapsed time between the present time and the generation time of the latest data packet at source, which allows us to effectively measure the information timeliness of the received data packets at the destination. Research that focuses on minimizing AoI plays an important role in multiple applications such as intelligent transportation systems, public safety networks, mission-critical systems, and industrial automation. For example, it is shown in [4] and [5] that, the timely updating of the speed and acceleration information of adjecent vehicles can be used to prevent potential accidents by taking timely actions.

NOMA is considered as an important candidate for future multiple access technologies. Compared with traditional orthogonal multiple access (OMA), NOMA allows multiple users to share the same resources, in which the successive interference cancellation (SIC) is applied to handle multiple access interference. In [6], NOMA and OMA schemes were compared with each other to demonstrate the significant advantage of NOMA transmission in spectrum resource utilization. In practical transmission, there are often limitations such as terrain and channel fading that result in poor channel conditions between the source node and the target user. To address this issue, cooperative communications are recommended [7], in which users with good channel conditions act as relays to forward data for users with poor channel conditions. This approach overcomes the absence of a direct transmission link between the sender and receiver, significantly improving the transmission performance. Cooperative NOMA has a wide range of application scenarios. In [8], the use of secondary users as relays is studied to improve the diversity order of users in cooperative NOMA scenarios. In [9], it was shown that, the use of dedicated relays in NOMA systems can better improve system coverage and transmission reliability. In [10]-[11], AoI minimization in wireless broadcast networks was studied. In [10], a Markov decision process (MDP) was established, and a hierarchical ON/OFF scheduling algorithm was proposed to minimize the average AoI. In [11], multiple low-complexity algorithms were proposed to minimize the expected weighted sum AoI of the network. However, previous research assumed the existence of a direct link between the source and destination nodes. Meanwhile, *generate-at-will* data generation model was assumed. There is still no research results on the minimum realized AoI for relaying scheme in buffer-aided wireless-powered NOMA network with random arrivals. And this is exactly the research motivations of our work in this paper.

In this paper, we focus on a buffer-aided wireless powered

979-8-3503-7099-7/24/$31.00 ©2024 IEEE

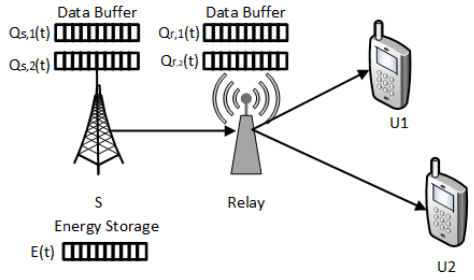

Fig. 1. Wireless powered downlink NOMA relay network

NOMA network, which comprises of one buffer-aided source node, one buffer-aided relay node, and two destination nodes. The source node is supposed to generates two data streams randomly and independently for two destination nodes, which can be buffered at source node temporarily before being transmitted later on. The relay node, on one hand, is supposed to provide energy supply to the source node through wireless energy harvesting technology, where the source node can store the collected energy in its energy storage. On the other hand, the relay can receive and buffer two data streams from source node intended for two destination nodes, and forward them to two destination nodes through downlink NOMA technology when scheduled. For this buffer-aided wireless powered NOMA network, the long-term weighted average AoI minimization problem for two destination nodes was formulated. By using Lyapunov optimization framework to solve the long-term weighted average AoI minimization problem, we obtain an adaptive AoI-aware relaying scheme. Our analysis results indicate that, by adaptively adjusting transmission rate, transmit power, and optimizing the transmission mode selection based on the buffer state information (BSI) of the source node and relay node, channel state information (CSI) of the source-relay link, the relay-destination links, and energy-consumption state information (ESI) of the source node and relay node, the long-term weighted average AoI performance at two destination nodes can be optimized. In addition, numerical analysis results are presented to show that, when compared with the traditional downlink NOMA relay network and the downlink time division multiple access (TDMA) relay network, the proposed AoI-aware adaptive relaying design in buffer-aided wireless powered NOMA relay network can realize smaller AoI.

The remainder of the paper is organized as follows. The buffer-aided wireless-powered NOMA relay network model and the long-term weighted average AoI minimization problem formulation were presented in Section II. The AoI-aware adaptive relaying scheme in buffer-aided wireless-powered NOMA network was derived in Section III. Numerical analysis results are presented in Section IV. Finally, we conclude our work in Section V.

II. System Model and Problem Formulation

A. System Model

As shown in Fig. 1, let us consider a time slotted downlink NOMA relay network consisting of one source S, one relay R, and two users U_1, U_2. We assume that S is provisioned with two data buffers $Q_{s,1}, Q_{s,2}$ to temporarily store data from either upper layer applications or sensors for U_1, U_2. Meanwhile, we assume that S is equipped with an energy storage E to store the collected energy from R. We assume no direct link between two users and S, hence their data must be relayed by R to two users in a half-duplex mode. R is supposed to provide wireless energy harvesting to S. In addition, R is provisioned with two data buffers $Q_{r,1}, Q_{r,2}$ to store two data streams intended for U_1, U_2. Without statement, all data buffers at S and R are assumed to operate in a *first-come first-served* (FCFS) queueing policy. All nodes are assumed to be provisioned with single antenna. The channels are assumed to be block-fading, such that the channel coefficients remain unchanged within one single time slot, but may change from one slot to another. Because buffer-aided transmission is assumed at S and R, we assume no packet loss during data transmission. The data arrival rates at S for U_1, U_2 within the t-th time slot are denoted as $\lambda_i(t), i \in \{1, 2\}$ and they follow a Bernoulli distribution. When there is no confusion, we let $Q_{s,1}(t), Q_{s,2}(t), Q_{r,1}(t), Q_{r,2}(t)$ represent the data buffer backlog sizes within the t-th time slot at S and R. In this paper, we assume that perfect CSI can be acquired by using channel estimate scheme. The influence of imperfect CSI on the realized performance will be left for future exploration. The channel coefficients $\tilde{h}(t)$, $\tilde{g}_1(t)$, and $\tilde{g}_2(t)$ represent the channel coefficients of the S-R link, the R-U_1 link and the R-U_2 link in the t-th time slot.

Let $q_i(t) \in \{0, 1\}, i \in \{1, 2, 3\}$ denote three mode indicators. $q_1(t) = 1$ indicates that S harvests energy from R. $q_2(t) = 1$ represents data transmission from S to R, while $q_3(t) = 1$ stands for the NOMA transmission from R to both users. Since the system is assumed to operate in half-duplex mode, only one mode can be selected in any time slot, i.e.,

$$\sum_{i=1}^{3} q_i(t) = 1. \tag{1}$$

When $q_1(t) = 1$, the harvested energy at S can be given by

$$E_h(t) = q_1(t) \frac{P_r(t) \left|\tilde{h}(t)\right|^2 \eta T}{d_{sr}^m}, \tag{2}$$

where T is the time slot duration, $P_r(t)$ represents the transmit power at R, d_{sr} is the distance between S and R, m is the path loss exponent, and $\eta \in [0, 1]$ represents the energy conversion efficiency. When $q_2(t) = 1$, the signal received at R is:

$$y_r(t) = \frac{\tilde{h}(t)}{\sqrt{d_{sr}^m}} \sqrt{P_s(t)} x_s(t) + n_r(t), \tag{3}$$

where $x_s(t)$ represents the signal transmited from S, and $E|x_s(t)|^2 = 1$. $n_r(t)$ is additive white Gaussian noise with zero mean and variance of σ^2 at R. In this scenario, the maximum transmission rate from S to R can be given by $\frac{1}{2}\log_2\left(1 + \frac{P_s(t)h(t)}{\sigma^2}\right)$, where $h(t) = \frac{\left|\tilde{h}(t)\right|^2}{d_{sr}^m}$. Let $R_{s,1}(t)$ and $R_{s,2}(t)$ denote the data rates intended for U_1 and U_2,

respectively, we have

$$R_{s,1}(t) + R_{s,2}(t) \leq q_2(t) log_2\left(1 + \frac{P_s(t)\, h(t)}{\sigma^2}\right). \quad (4)$$

When $q_3(t) = 1$, R will forward two data streams to both users in a NOMA manner, namely, it will transmit the following signal to two users:

$$x_r(t) = \sqrt{P_{r,1}(t)}x_1(t) + \sqrt{P_{r,2}(t)}x_2(t), \quad (5)$$

where $x_i(t), i \in \{1,2\}$ represents the signals intended for U_i, and $E|x_i(t)|^2 = 1$. $P_{r,i}(t)$ stands for the allocated transmit powers for U_i. Hence, the signal received at U_i can be given by:

$$y_i(t) = \frac{\tilde{g}_i(t)}{\sqrt{d_{ri}^m}} x_r(t) + n_{i,u}(t), \quad (6)$$

where $d_{ri}(i = 1, 2)$ represents the distance from R to U_i, and $n_{i,u}(t)$ is noise at U_i with zero-mean and variance σ^2. When $\frac{|\tilde{g}_1(t)|^2}{d_{r1}^m} < \frac{|\tilde{g}_2(t)|^2}{d_{r2}^m}$, let $R_{r,i}(t)$ represents the achievable rate on R-U_i link, we have:

$$R_{r,1}(t) = q_3(t) \log_2\left(1 + \frac{P_{r,1}(t)\, g_1(t)}{g_1(t)\, P_{r,2}(t) + \sigma^2}\right), \quad (7)$$

$$R_{r,2}(t) = q_3(t) \log_2\left(1 + \frac{g_2(t)\, P_{r,2}(t)}{\sigma^2}\right), \quad (8)$$

where $g_i(t) = \frac{|\tilde{g}_i(t)|^2}{d_{ri}^m}$. The maximum transmit powers at S and R are $\hat{P}_s$ and $\hat{P}_r$, respectively. The average transmit power by R is assumed to be $\bar{P}_r$. Since S harvests energy from R and stores the collected energy in its energy storage, we have $\hat{P}_s(t) = \frac{E(t)}{T}$, where $E(t)$ represents the energy status of the energy storage in time slot t. Then we have:

$$P_s(t) \leq \hat{P}_s(t), \quad (9)$$

$$P_{r,1}(t) + P_{r,2}(t) \leq \hat{P}_r. \quad (10)$$

B. AoI Evolution

Let $N_1(t)$ and $N_2(t)$ stand for the total number of data packets generated for U_1 and U_2 at S till time slot t. L_1 and L_2 represent the packet sizes for U_1 and U_2, respectively. $U_1(t) = \{u_{1,1}(t), \cdots, u_{1,N_1(t)}(t)\}, U_2(t) = \{u_{2,1}(t), \cdots, u_{2,N_2(t)}(t)\}$ represent the generation time of $N_1(t)$ and $N_2(t)$ packets. The AoI $X_1(t)$ and $X_2(t)$ at U_1 and U_2 in time slot t are given by

$$X_1(t) = t - u_{1,W_1(t)}(t), \quad (11)$$

$$X_2(t) = t - u_{2,W_2(t)}(t). \quad (12)$$

where $W_1(t)$ and $W_2(t)$ represents the total number of data packets received by U_1 and U_2 till time slot t, which can be calcualted as below

$$W_1(t) = \left\lfloor \frac{Q_1(t)}{L_1} \right\rfloor, \quad (13)$$

$$W_2(t) = \left\lfloor \frac{Q_2(t)}{L_2} \right\rfloor. \quad (14)$$

where $Q_1(t)$ and $Q_2(t)$ represents the total number of data bits received by U_1 and U_2 till time slot t.

C. Problem Formulation

Our objective is to minimize the long-term weighted average AoI for both users while maintaining the stability of all data queues and energy queues. The long-term weighted average AoI minimization problem can be formulated as follows:

$$\textbf{P1:} \min_{\boldsymbol{\mathcal{R}}(t), P_s(t), \boldsymbol{\mathcal{P}_r}(t), \boldsymbol{q}(t)} \lim_{t\to\infty} \frac{1}{t} \sum_{t=0}^{t-1} (\alpha X_1(t) + (1-\alpha) X_2(t))$$

$$\text{s.t.} \quad C1: Q_{s,i}(t+1) = (Q_{s,i}(t) + \lambda_i(t) - R_{s,i}(t))^+, i = 1, 2,$$

$$C2: Q_{r,i}(t+1) = (Q_{r,i}(t) + R_{s,i}(t) - R_{r,i}(t))^+, i = 1, 2,$$

$$C3: E(t+1) = \min\left(E(t) + E_h(t) - E_s(t), \hat{E}\right),$$

$$C4: Z(t+1) = \left(Z(t) + \sum_{i=1}^{2} P_{r,i}(t) - \bar{P}_r\right)^+,$$

$$C5: Q_i(t+1) = Q_i(t) + R_{r,i}(t), i = 1, 2,$$

$$C6: X_i(t) = t - u_{i,W_i(t)}(t), \quad i = 1, 2,$$

$$C7: \lim_{M\to\infty} \frac{1}{M} \sum_{t=0}^{M-1} R_{s,i}(t) \geq \lambda_i(t), i = 1, 2$$

$$\lim_{M\to\infty} \frac{1}{M} \sum_{t=0}^{M-1} R_{r,i}(t) \geq \lim_{M\to\infty} \frac{1}{M} \sum_{t=0}^{M-1} R_{s,i}(t), i = 1, 2$$

$$C8: R_{s,1}(t) + R_{s,2}(t) \leq q_2(t) \log_2\left(1 + \frac{P_s(t) h(t)}{\sigma^2}\right),$$

$$C9: P_s(t) \leq \hat{P}_s$$

$$C10: P_r(t) \leq \hat{P}_r$$

$$C11: P_{r,1}(t) + P_{r,2}(t) \leq \hat{P}_r(t)$$

$$C12: q_i(t) \in \{0, 1\}, i \in \{1, 2, 3\}$$

$$C13: q_1(t) + q_2(t) + q_3(t) = 1$$

$$C14: (R_{r,1}(t), R_{r,2}(t))$$

$$= \begin{cases} q_3(t)\left(\log_2\left(1 + \frac{P_{r,1}(t) g_1(t)}{g_1(t) P_{r,2}(t) + \sigma^2}\right), \right. \\ \left. q_3(t) \log_2\left(1 + \frac{g_2(t) P_{r,2}(t)}{\sigma^2}\right)\right) \text{ if } g_1(t) < g_2(t) \\ q_3(t)\left(\log_2\left(1 + \frac{g_1(t) P_{r,1}(t)}{\sigma^2}\right), \right. \\ \left. q_3(t) \log_2\left(1 + \frac{P_{r,2}(t) g_2(t)}{g_2(t) P_{r,1}(t) + \sigma^2}\right)\right) otherwise \end{cases}$$

where $\boldsymbol{\mathcal{R}}(t) = \{R_{s,1}(t), R_{s,2}(t), R_{r,1}(t), R_{r,2}(t)\}$, $\boldsymbol{\mathcal{P}_r}(t) = \{P_{r,1}(t), P_{r,2}(t)\}$, $\boldsymbol{q}(t) = \{q_1(t), q_2(t), q_3(t)\}$. $E_s(t) = q_2(t)(P_{s,1}(t) + P_{s,2}(t))T$ represents the energy consumption at S in time slot t. $\hat{P}$ and $\hat{P}_s(t)$ represent the peak transmit power constraint at R and S, respectively. Due to the constraint that the energy used for transmission at S cannot exceed the energy stored in its energy storage, we have $\hat{P}_s(t) = \frac{E(t)}{T}$. $C1$ and $C2$ represent data buffer update constraints at S and R,

respectively. $C3$ is the virtual energy queue update constraint at S. $C4$ is the virtual power queue update constraint at R. $C5$ and $C6$ represent the AoI evolution constraints at users. $C7$ represents the target rate constraints for both users. $C8$ ensures that the transmission rate from S to R does not exceed its link capacity. $C9$ is the peak transmit power constraint at S. $C10$ and $C11$ are the peak transmit power constraints at R. $C12$ and $C13$ are transmission mode selection constraints in each time slot. $C14$ represents the power allocation constraint at R.

III. Adaptive Transmission Scheme Design

Since **P1** is a non-convex time average optimization problem that is difficult to solve directly. In this section, we transform the time average optimization problem into real-time problem by employing the Lyapunov optimization framework, and decompose it into three subproblems to derive the optimal rate allocation, power allocation, and transmission mode selection separately. For the data buffers at S and R, we have the following **Lemma 1**.

Lemma 1: If all data queues $Q_{s,i}(t)$ and $Q_{r,i}(t), i \in \{1,2\}$ are rate-stable, i.e., $\lim_{M\to\infty}\frac{Q_{s,i}(t)}{M}=\lim_{M\to\infty}\frac{Q_{r,i}(t)}{T}=0$, we have

$$\lim_{M\to\infty}\frac{1}{M}\sum_{t=0}^{M-1}R_{s,i}(t)\geq\lambda_i(t), \tag{15}$$

$$\lim_{M\to\infty}\frac{1}{M}\sum_{t=0}^{M-1}R_{r,i}(t)\geq\lim_{M\to\infty}\frac{1}{M}\sum_{t=0}^{M-1}R_{s,i}(t). \tag{16}$$

Proof: Based on $C1$, $C2$ of **P1**, we have

$$Q_{s,i}\left(t+1\right)\geq Q_{s,i}\left(t\right)+\lambda_i\left(t\right)-R_{s,i}\left(t\right), \tag{17}$$

$$Q_{r,i}\left(t+1\right)\geq Q_{r,i}\left(t\right)+R_{s,i}\left(t\right)-R_{r,i}\left(t\right). \tag{18}$$

Without loss of generality, we assume zero initial data queues, namely, $Q_{s,i}(0)=Q_{r,i}(0)=0$. Since all data queues are rate stable, i.e., $\lim_{M\to\infty}\frac{Q_{s,i}(t)}{M}=\lim_{M\to\infty}\frac{Q_{r,i}(t)}{T}=0$, by substituting them into (14) and (15), we can obtain **Lemma 1**. According to **Lemma 1**, we know that $C7$ can be satisfied if all data queues are rate stable. Thus, the original problem **P1** can be transformed into the problem of minimizing the AoI for two users while ensuring the stability of data, energy, and virtual power consumption queues. The Lyapunov optimization framework can thus be used to effectively handle this issue. Let us define the following quadratic Lyapunov function:

$$\begin{aligned}L(\boldsymbol{\Theta}(t))=&\frac{\mu_1}{2}Q_{s,1}^2(t)+\frac{\mu_2}{2}Q_{s,2}^2(t)+\frac{\mu_3}{2}Q_{r,1}^2(t)\\&+\frac{\mu_4}{2}Q_{r,2}^2(t)+\frac{\mu_5}{2}(\hat{E}-E(t))^2+\frac{\mu_6}{2}Z(t)^2,\end{aligned} \tag{19}$$

where $\boldsymbol{\Theta}(t)=[Q_{s,1}(t),Q_{s,2}(t),Q_{r,1}(t),Q_{r,2}(t),E(t),Z(t)]$ denotes the concatenated queue vector, $\{\mu_i,i=1,2,3,4,5,6\}$ are non-negative weighting coefficients, which are used to ensure that the data buffer, energy storage, virtual power queues are magnitude comparable. Then the Lyapunov drift function can be given by

$$\Delta(\Theta(t))=E[L(\Theta(t+1))-L(\Theta(t))|\Theta(t)]. \tag{20}$$

Now minimizing the long-term weighted average AoI can be transferred to minimizing the following Lyapunov drift-plus-penalty function:

$$\Delta(\Theta(t))+VE[\alpha X_1(t)+(1-\alpha)X_2(t)|\Theta(t)], \tag{21}$$

where V is a non-negative weighting parameter used to adjust the tradeoff between queue size and throughput.

Lemma 2: The upper bound of the Lyapunov drift-plus-penalty function can be given by:

$$\begin{aligned}&\Delta(\Theta(t))+VE[\alpha X_1(t)+(1-\alpha)X_2(t)|\Theta(t)]\\\leq&\mathcal{B}+VE[\alpha X_1(t)+(1-\alpha)X_2(t)|\Theta(t)]+\\&\mu_1Q_{s,1}(t)E[\lambda_1(t)-R_{s,1}(t)|\Theta(t)]+\\&\mu_2Q_{s,2}(t)E[\lambda_2(t)-R_{s,2}(t)|\Theta(t)]+\\&\mu_3Q_{r,1}(t)E[R_{s,1}(t)-R_{r,1}(t)|\Theta(t)]+\\&\mu_4Q_{r,2}(t)E[R_{s,2}(t)-R_{r,2}(t)|\Theta(t)]+\\&\mu_5(\hat{E}-E(t))E[E_s(t)-E_h(t)|\Theta(t)]+\\&\mu_6Z(t)E[(P_{r,1}(t)+P_{r,2}(t)-\bar{P}_r)|\Theta(t)],\end{aligned} \tag{22}$$

where the constant $\mathcal{B}$ is given by

$$\begin{aligned}\mathcal{B}=&\frac{\mu_1}{2}\hat{R}_{s,1}^2\left(t\right)+\frac{\mu_2}{2}\hat{R}_{s,2}^2\left(t\right)+\frac{\mu_3}{2}\hat{R}_{s,1}^2\left(t\right)+\\&\frac{\mu_3}{2}\hat{R}_{r,1}^2\left(t\right)+\frac{\mu_4}{2}\hat{R}_{s,2}^2\left(t\right)+\frac{\mu_4}{2}\hat{R}_{r,2}^2\left(t\right)+\\&\frac{\mu_5}{2}\left(\hat{E}_s^2\left(t\right)+\hat{E}_h^2\left(t\right)\right)+\mu_6\hat{P}_r^2\left(t\right).\end{aligned} \tag{23}$$

where $\hat{R}_{s,1}\left(t\right),\hat{R}_{s,2}\left(t\right),\hat{R}_{r,1}\left(t\right),\hat{R}_{r,2}\left(t\right)$ represent the maximum transmission rates intended for two users at S and R, respectively. $\hat{E}_s\left(t\right),\hat{E}_h\left(t\right)$ represents the maximum energy consumed and harvested by S. $\hat{P}_r(t)$ represent the maximum power consumed at R. In this paper, we aim to obtain an online adaptive transmission scheme to minimize the upper bound of the Lyapunov drift plus penalty in (19) via rate allocation, power allocation, and transmission mode selection, as illustrated by the following real-time optimization problem:

$$\begin{aligned}\mathbf{P2}:\min_{\boldsymbol{\mathcal{R}}(t),P_s(t),\boldsymbol{\mathcal{P}_r}(t),\boldsymbol{q}(t)}\quad&V\left(\alpha X_1(t)+(1-\alpha)X_2(t)\right))\\&+\mu_1Q_{s,1}(t)(-R_{s,1}(t))+\mu_2Q_{s,2}(t)(-R_{s,2}(t))\\&+\mu_3Q_{r,1}(t)(R_{s,1}(t)-R_{r,1}(t))+\mu_4Q_{r,2}(t)(R_{s,2}(t)-R_{r,2}(t))\\&+\mu_5(\hat{E}-E(t))(E_s(t)-E_h(t))+\mu_6Z(t)\left(\sum_{i=1}^{2}P_{r,i}(t)-\bar{P}_r\right)\\\text{s.t.}\quad&C5,C6,C8\sim C14.\end{aligned} \tag{24}$$

P2 can be further subdivided into the following three subproblems. Firstly, in energy harvesting mode, i.e., $q_1(t)=1$, the optimization problem **P2** can be equivalently transformed into **P3**:

$$\begin{aligned}\mathbf{P3:}\min_{\boldsymbol{\mathcal{P}_r}(t)}\quad&\left\{-\mu_5(\hat{E}-E(t))P_r(t)h(t)\eta T+V\left(\alpha X_1(t)\right.\right.\\&\left.\left.+(1-\alpha)X_2(t)\right)\right\}\\\text{s.t.}\quad&C10.\end{aligned} \tag{25}$$

Apparently, the above optimization problem is a standard linear programming problem. Thus, we can obtain the optimal power allocation of the relay in the energy harvesting mode,

which is $P_r(t) = \hat{P}_r$. In the relay receiving mode, i.e., $q_2(t) = 1$, the optimization problem **P2** can be equivalently transformed into **P4**.

$$\begin{aligned}\textbf{P4:}\ &\min_{R_{s,1}(t),R_{s,2}(t),P_s(t)} \mu_1 Q_{s,1}(t)(-R_{s,1}(t)) + \mu_2 Q_{s,2}(t)(-R_{s,2}(t)) \\ &+ \mu_3 Q_{r,1}(t) R_{s,1}(t) + \mu_4 Q_{r,2}(t) R_{s,2}(t) \\ &+ V(\alpha X_1(t) + (1-\alpha) X_2(t)) + \mu_5(\hat{E} - E(t)) P_s(t) T \\ &\text{s.t.}\ \ C8, C9.\end{aligned} \tag{26}$$

P4 is a standard convex optimization problem, hence we can easily obtain the following optimal rate and power allocation by using the KKT (Karush-Kuhn-Tucher) conditions

$$(R^*_{s,1}(t), R^*_{s,2}(t)) = \begin{cases} \left(log_2\left(1 + \frac{P_s(t)h(t)}{\sigma^2}\right), 0\right), \\ \text{if} \quad D_1(t) \geq D_2(t)\ \&\ D_1(t) > 0 \\ \left(0, log_2\left(1 + \frac{P_s(t)h(t)}{\sigma^2}\right)\right), \\ \text{if} \quad D_2(t) \geq D_1(t)\ \&\ D_2(t) > 0 \\ (0,0), \text{otherwise.} \end{cases} \tag{27}$$

$$P^*_s(t) = \begin{cases} \min\left(\left(\frac{D_1(t)}{\mu_5 * \left(\hat{E} - E(t)\right) * T * ln2} - \frac{\sigma^2}{h(t)}\right)^+, E(t)/T\right), \\ \text{if} D_1(t) \geq D_2(t) \& D_1(t) > 0 \\ \min\left(\left(\frac{D_2(t)}{\mu_5 * \left(\hat{E} - E(t)\right) * T * ln2} - \frac{\sigma^2}{h(t)}\right)^+, E(t)/T\right), \\ \text{if} D_2(t) \geq D_1(t)\ \&\ D_2(t) > 0 \\ 0, \text{otherwise.} \end{cases} \tag{28}$$

where $D_1(t) = \mu_1 Q_{s,1}(t) - \mu_2 Q_{r,1}(t)$, $D_2(t) = \mu_3 Q_{s,2}(t) - \mu_4 Q_{r,2}(t)$. From (27), we can observe that the optimal transmission rates are dependent on the data buffer backlog differences between S and R, as well as the CSI. When the weighted backlog at R ($\mu_1 Q_{s,1}(t)$ and $\mu_3 Q_{s,2}(t)$) is larger than the weighted backlog at S ($\mu_2 Q_{r,1}(t)$ and $\mu_4 Q_{r,2}(t)$), S will not transmit. In fact, one may readily notice that, the optimal transmission over S-R link tends to be a time division transmission.

When R is scheduled to transmit data to both users, i.e., $q_3(t) = 1$, without loss of generality, we assume that $g_1(t) < g_2(t)$, and the results can be easily extended to the case of $g_1(t) > g_2(t)$. The optimization problem **P2** can be equivalently transformed into the following **P5**

$$\begin{aligned}\textbf{P5:}\ &\min_{R_{r,1}(t),R_{r,2}(t),P_{r,1}(t),P_{r,2}(t)} -\mu_2 Q_{r,1}(t) R_{r,1}(t) - \\ &\mu_4 Q_{r,2}(t) R_{r,2}(t) + V(\alpha X_1(t) + (1-\alpha) X_2(t)) \\ &+ \mu_6 Z(t)(P_{r,1}(t) + P_{r,2}(t)) \\ &\text{s.t.}\ \ C5, C6, C11, C14.\end{aligned} \tag{29}$$

From (11) and (12), it can be noted that the AoI evolution is linearly negatively correlated with the transmission rates $R_{r,1}(t)$ and $R_{r,2}(t)$, as well as the packet lengths L_1 and L_2. This correlation can be used to represent the variation in AoI to obtain suboptimal solutions. However, even with this linear correlation, **P5** is still not a convex optimization problem. From $C14$, we can obtain

$$P^*_{r,1}(t) = \left(2^{R_{r1}(t)} - 1\right)\left(\frac{2^{R_{r,2}(t)}\sigma^2}{g_2(t)} + \frac{\sigma^2}{g_1(t)} - \frac{\sigma^2}{g_2(t)}\right), \tag{30a}$$

$$P^*_{r,2}(t) = \left(2^{R_{r,2}(t)} - 1\right)\frac{\sigma^2}{g_2(t)}. \tag{30b}$$

By substituting (30) into **P5**, we can obtain the following equivalent optimization problem

$$\begin{aligned}\textbf{P6:}\ &\min_{R_{r,1}(t),R_{r,2}(t)} -\mu_2 Q_{r,1}(t) R_{r,1}(t) - \mu_4 Q_{r,2}(t) R_{r,2}(t) + \\ &V(\alpha X_1(t-1) + (1-\alpha) X_2(t-1)) \\ &-\left(\frac{V\alpha}{L_1} R_{r,1}(t) + \frac{V(1-\alpha)}{L_2} R_{r,2}(t)\right) + \\ &\mu_6 Z(t)\sigma^2\left(\frac{2^{R_{r,1}(t)+R_{r,2}(t)}}{g_2(t)} - \frac{1}{g_1(t)}\right) \\ &+\mu_6 Z(t)\sigma^2\left(\frac{1}{g_1(t)} - \frac{1}{g_2(t)}\right)2^{R_{r,1}(t)} \\ &\text{s.t.}\sigma^2\left(\frac{2^{R_{r,1}(t)+R_{r,2}(t)}}{g_2(t)} + \left(\frac{1}{g_1(t)} - \frac{1}{g_2(t)}\right)2^{R_{r,1}(t)} - \frac{1}{g_1(t)}\right) \\ &\leq \hat{P}_r.\end{aligned} \tag{31}$$

One can observe that **P6** is convex. Hence, we can obtain the following optimal rate allocation by using the KKT conditions

$$(R^*_{r,1}, R^*_{r,2}) = \begin{cases} \left(log_2\left(\frac{\mu_1(Q_{r,1}-Q_{r,2})}{\mu_6 Z\sigma^2\left(\frac{1}{g_1}-\frac{1}{g_2}\right)ln2}\right), log_2\left(\frac{\mu_1 Q_{r,2}(g_2-g_1)}{\mu_1(Q_{r,1}-Q_{r,2})g_1}\right)\right) \\ \text{if} \quad m_1 > m_2, m_3 > 0, \beta < 0, \\ \left(log_2\left(\frac{\mu_2 Q_{r,1}-\mu_4 Q_{r,2}}{(\mu_6 Z+\beta)\sigma^2\left(\frac{1}{g_1}-\frac{1}{g_2}\right)ln2}\right), log_2\left(\frac{\mu_4 Q_{r,2}(g_2-g_1)}{(\mu_2 Q_{r,1}-\mu_4 Q_{r,2})g_1}\right)\right) \\ \text{if} \quad m_5 > 0, m_3 > 0, \beta \geq 0, \\ \left(log_2\left(\frac{\mu_2 Q_{r,1} g_1}{\mu_6 Z\sigma^2 ln2}\right), 0\right) \quad \text{if} \quad m_1 > 0, m_3 \leq 0, \beta < 0, \\ \left(log_2\left(1 + \frac{\widehat{P}_r g_1}{\sigma^2}\right), 0\right) \quad \text{if} \quad m_3 \leq 0, \beta \geq 0, \\ \left(0, log_2\left(\frac{\mu_4 Q_{r,2} g_2}{\mu_6 Z\sigma^2 ln2}\right)\right) \quad \text{if} \quad m_1 \leq m_2, m_2 > 0, m_4 < 0, \\ \left(0, log_2\left(1 + \frac{\widehat{P}_r g_2}{\sigma^2}\right)\right) \quad \text{if} \quad m_5 \leq 0, m_4 \geq 0, \\ (0,0), \text{otherwise.} \end{cases} \tag{32}$$

$$\begin{aligned} &m_1 = \mu_2 Q_{r,1} - \frac{\mu_6 Z\sigma^2 ln2}{g_1}, m_2 = \mu_4 Q_{r,2} - \frac{\mu_6 Z\sigma^2 ln2}{g_2} \\ &m_3 = \mu_4 Q_{r,2} g_2 - \mu_2 Q_{r,1} g_1, \\ &m_4 = \mu_4 Q_{r,2} - \frac{\mu_6 Z\left(\widehat{P}_r g_2 + \sigma^2\right) ln2}{g_2}, \\ &m_5 = \mu_2 Q_{r,1}\left(\widehat{P}_r + \frac{\sigma^2}{g_2}\right) - \mu_4 Q_{r,2}\left(\widehat{P}_r + \frac{\sigma^2}{g_1}\right), \\ &\beta = \frac{\mu_2 Q_{r,1} g_1}{\left(\widehat{P_r} g_1 + \sigma^2\right) ln2} - \mu_6 Z \end{aligned}$$

From (32), we can see that the optimal transmission rate allocation at R are dependent on the backlog at R, channel conditions, and the average power. Unlike traditional power

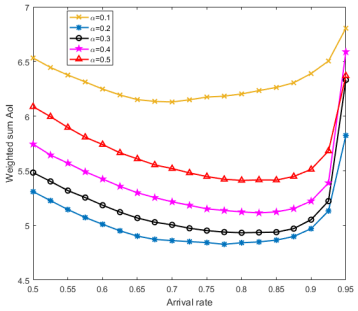

Fig. 2. Realized AoI performance of two users with different arrival rates.

water-filling algorithms, it is evident that in the power allocation, users with larger backlogs will be allocated with more power allocation. This is because AoI is highly sensitive to backlog, so the optimal scheme will increase the transmit power for user with relatively larger backlog to reduce its AoI.

Let $A(t) = \{A_1(t), A_2(t), A_3(t)\}$ denote the utility function vector for three modes, whose values correspond to the optimal value of the optimization problem in (25), (26), and (29), respectively.

$$q_k^*(t) = 1, if A_k(t) = \arg \min_{i \in \{1,2,3\}} A_i(t). \tag{33}$$

IV. Numerical Analysis

we will evaluate the realized performance of the proposed adaptive AoI-aware relaying scheme in buffer-aided wireless powered NOMA relay network by using Monte Carlo simulations. In all simulations, the following parameters are assumed. The noise variances $\sigma_a^2 = \sigma_c^2 = -63dBm$. The energy storage size is $E = 1J$, the peak transmit power at R is $\bar{P}_r = 2W$, and the average transmit power is $\bar{P}_r = 5mW$. We assume that all link path loss exponents are set to $m = 2.7$. We assume that the average power attenuation of the signal at a reference distance of $1m$ is $30dB$. The weighting coefficients $\mu_1 = \mu_2 = \mu_3 = \mu_4 = 1$, $\mu_5 = 10^5$, and $\mu_6 = 10^6$. The energy conversion efficiency is $\eta = 0.5$. The normalized packet size $L_1 = L_2 = 4$. $d_{sr} = 25m$, $d_{r1} = 20m$ and $d_{r2} = 25m$, namely, U_1 is assumed to be a user with better link to R. The duration of each time slot is normalized to unity. All simulation results are obtained over $T = 10^6$ time slots.

The weighted sum AoI performance is illustrated in Fig. 2 for two users with different AoI weighting coefficient α for U_1. One can readily observe that, different α will lead to quite different weighted sum AoI performance. With the increase in α, the weighted sum AoI performance will first improve and then degrade. In fact, α represents the relative AoI performance preference by U_1. When $\alpha = 0.1$, the system lays emphasis on the AoI performance of U_2, which requires more resource should be allocated to U_2. U_2 has an inferior link to R, thus the overall weighted sum AoI performance is not so good. With the increase in α, the system will gradually allocate more resources to U_1, which leads to the improved weighted sum AoI performance. In fact, we can see that the minimum weighted sum AoI can be realized when $\alpha = 0.2$.

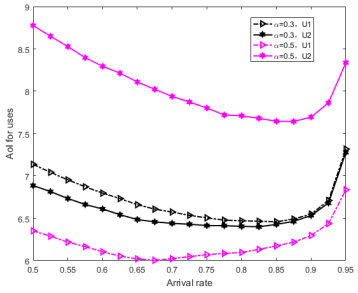

Fig. 3. The influence of AoI weighting coefficient α on the realized AoI performance.

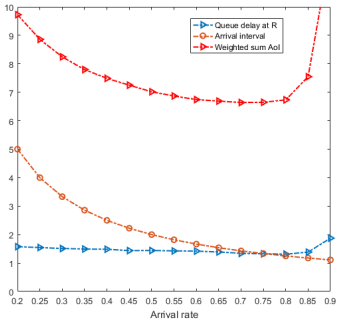

Fig. 4. The optimal arrival rate illustration, $\alpha = 0.5$, $d_{sr} = d_{r1} = d_{r2} = 25m$.

With the further increase of α from 0.2 to 0.5, the system tends to allocate more resource to U_1, leading to increased backlog for U_2, which explicates the degraded weighted sum AoI performance when $\alpha \in [0.2, 0.5]$. In order to better illustrate how the AoI weighting coefficient α affect the realized AoI performance, we illustrate the AoI performance for U_1 and U_2 in Fig. 3. As illustrated in Fig.3, when $\alpha = 0.5$, both users have the same AoI performance requirements. In this case, U_1 can realize much better AoI performance than U_2. However, U_2 might have a more strict requirements on the realized AoI performance. In fact, by letting $\alpha = 0.3$, we can noticeably improve the AoI performance for U_2, which is even better than U_1, even U_1 has a better link to R. This confirms us that the proposed AoI adaptive transmission scheme can flexibly meet different AoI requirements by properly adjusting α.

One may also note the existence of an optimal arrival rate in terms of the realized minimum weighted sum AoI performance. In order to explicate this phenomena, we illustrate the average sum AoI in Fig. 4 for a symmetric case, where $d_{sr} = d_{r1} = d_{r2} = 25m$, $\alpha = 0.5$. One can notice that, the optimal arrival rate corresponds to the intersection between the arrival interval and the queuing latency at R. Basically, the end-to-end AoI performance is dependent on three factors of the data generation interval, the queuing latency and transmission delay. For the two-hop transmission scheme, the transmission delay for each data packet from S is two time slots. Hence, the variations in data generation interval and queuing delay explicate the variations in the realized AoI performance. From (27), one can see that, the queue backlog at S is always greater than that at E. Obviously, under stable data buffer conditions at S and R, the queuing latency at

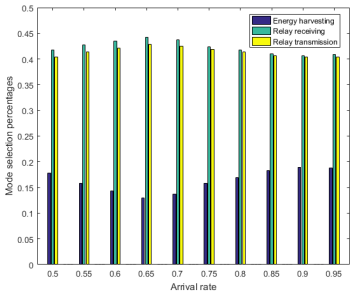

Fig. 5. Illustration of adaptive transmission mode selection, $\alpha = 0.5$.

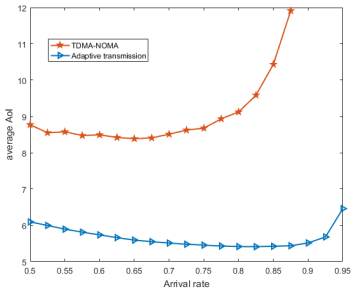

Fig. 6. Realized AoI performance of two users with different arrival rates.

R is always less than that at S, namely, the queuing delay variations in the queuing delay at R will be more noticeable for illustration purpose. Obviously, when the data generation interval is greater than the queuing delay, data generation interval will become the dominant factor for the realized AoI performance, which explicates the decrease in the weighted sum AoI performance when the arrival rate increases within small to moderate range. With the further increase in the arrival rate, the data backlog will increase as well. When the data generation interval becomes less than the queuing delay, now the dominant factor of the AoI performance will become the queuing delay. We can note that, the increase of the queuing delay will give rise to the increase in the realized weighted sum AoI performance, while the intersection point of the data generation interval and the queuing delay exactly corresponds to the optimal arrival rate at 0.75. The adaptive transmission mode selections with different arrival rates are illustrated in Fig. 5. One can note that, in order to minimize the AoI performance, only about 15% mode selection will be allocated to energy harvesting, while both relay receiving mode and relay transmitting mode are very close to each other, both of which are slightly greater than 0.4.

To verify the superiority of the proposed AoI aware adaptive transmission scheme, we include a TDMA-NOMA based scheme for comparison. In the TDMA-NOMA scheme, in the first time slot, S receives energy from R, in the second and third time slots, S transmits data intended for U_1 and U_2 to R, respectively. In the fourth and fifth time slots, R forwards the data that are temporarily stored at R to U_1 and U_2 through downlink NOMA technology, respectively. As shown in Fig. 6, the proposed adaptive transmission scheme noticeably outperforms the TDMA-NOMA based scheme in terms of the realized AoI performance for different arrival rates. This is because in the TDMA-NOMA scheme, S and R cannot adjust their transmission strategies promptly based on the queue backlog state, which results in larger queue backlogs. However, the adaptive transmission scheme can adjust its transmission strategy adaptively based on the underlying CSI, BSI, ESI, and the AoI state information (ASI), thereby achieving a better AoI performance.

V. Conclusion

In this paper, we focused on the problem of minimizing AoI in a wireless-powered NOMA network with buffer-aided relay. In this network, a buffer-aided source node is supposed to harvest energy from the relay to transmit its randomly two data streams to two users via a buffer-aided relay. By solving the long-term average weighted sum AoI minimization problem with the Lyapunov optimization framework, we have developed a buffer-aided adaptive transmission scheme. Numerical analysis results have demonstrated that, by adaptively adjusting the transmission rate, transmit powers, and optimizing the selection of appropriate transmission modes based on the the underlying CSI, BSI, ESI, and the ASI, the long-term weighted average AoI performance at two destination users can be effectively ensured. Meanwhile, different AoI requirements by different users can also be effectively supported by adjusting the AoI weighting coefficients. Our analysis results show that, the AoI-aware relaying scheme provides an effective adaptive relaying for buffer-aided wireless powered NOMA relay network.

References

[1] R. D. Yates, Y . Sun, D. R. Brown, S. K. Kaul, E. Modiano, and S. Ulukus, "Age of Information: An Introduction and Survey," *IEEE J. Sel. Areas Commun.*, vol. 39, no. 5, 2021.

[2] L. Huang and L. P. Qian, "Age of Information for Transmissions over Markov Channels," *Proc. of IEEE Globecom*, Singapore, 2017.

[3] S. Kaul, R. Yates and M. Gruteser, "Real-time Status: How Often Should One Update?" *Proc. of IEEE INFOCOM*, 2012.

[4] A. Validi, T. Ludwig, A. Hussein, and C. Olaverri-Monreal, "Examining the Impact on Road Safety of Different Penetration Rates of Vehicle-to-Vehicle Communication and Adaptive Cruise Control," *IEEE Intel. Trans. Syst. Mag.*, vol. 10, no. 4, pp. 24-34, 2018.

[5] S. Kaul, M. Gruteser, V. Rai, and J. Kenney, "Minimizing age of information in vehicular networks", *Proc. of the 8th Annu. IEEE Commun. Soc. Conf. Sens. Mesh Ad Hoc Commun. Netw.*, pp. 350-358, 2011.

[6] S. M. R. Islam, N. Avazov, O.A. Dobre and K. S. Kwak, "Power-Domain Non-Orthogonal Multiple Access (NOMA) in 5G Systems: Potentials and Challenges," *IEEE Communications Surveys & Tutorials*, vol. 19, no. 2, pp. 721-742, 2017.

[7] J. N. Laneman, D. N. C. Tse, G. W. Wornell, "Cooperative Diversity in Wireless Networks: Efficient Protocols and Outage Behavior," *IEEE Trans. Inform. Theory*, vol.50, no.12, pp.3062-3080, 2004.

[8] X. Yue, Y. Liu, S. Kang, et al, "Performance Analysis of NOMA with Fixed Gain Relaying over Nakagami-m Fading Channels," *IEEE Access*, vol.5, pp. 5445-5454, 2017.

[9] I. Kadota, E. Uysal-Biyikoglu, R. Singh, and E. Modiano, "Minimizing the Age of Information in Broadcast Wireless Networks," *54th Annual Allerton Conference on Communication, Control, and Computing* (Allerton), pp.844-851, 2016.

[10] Y. P. Hsu, E. Modiano, and L. Duan, "Scheduling Algorithms for Minimizing Age of Information in Wireless Broadcast Networks with Random Arrivals," *IEEE Trans. Mobile Comput.*, vol.19, no.12, 2020.

[11] I. Kadota, A. Sinha, E. Uysal-Biyikoglu, R. Singh, and E. Modiano, "Scheduling Policies for Minimizing Age of Information in Broadcast Wireless Networks," *IEEE/ACM Trans. Netw.*, vol. 26, no. 6, 2018.